

# EXPERIMENTAL STUDY ON PERMEABILITY OF A FRACTURE SUBJECT TO SHEAR DEFORMATION

Masao Goto

## 1. INTRODUCTION

Fracture surfaces in an underground rock are subjected to both normal and shear stresses since high compressive stress is applied to the rock. Since the permeability of a fracture depends on these stresses, the evaluation of the permeability of a fracture under compression is important for developing technologies for disposal of high-level radioactive wastes and hot dry rock (HDR) type geothermal energy extraction. A permeability test is often performed by a direct shear test in the laboratory. However, in a direct shear test, the normal stress on fracture surfaces is not uniform since a moment acts on the fracture surfaces. Therefore, the permeability of a fracture cannot be evaluated accurately by the direct shear test and furthermore, the evaluation of the heterogeneity in permeability is insufficient. To solve these problems, the permeability test system using a flat-jack type triaxial compressive test apparatus was developed (2005, Takamishi) [1]. However, there have been several problems in this system. Thus, this study aims to improve this experimental system and to evaluate the characteristics of the permeability of a rock fracture that is subject to shear displacement.

## 2. EXPERIMENTAL SYSTEM

### 2.1 OUTLINE OF THE SYSTEM

A flat-jack type triaxial compressive apparatus has been developed to solve the problems of a direct shear test and also to evaluate permeability of a fracture. Fig. 1 shows a schematic diagram of the experimental system. Fig. 2 shows the stress state in the experiment with the coordinate system. In the permeability test, first, water is injected into the fracture from the bottom of the specimen by a constant flow rate pump to exhaust air in the fracture. Then water is supplied to the top of the fracture until a steady-state flow condition is reached under a hydrostatic pressure. Afterward, the shear stress is increased while keeping the normal stress constant by controlling  $\sigma_z$  and  $\sigma_x$ . At several stages of shear displacement, the permeability of the fracture is evaluated by measuring water volume that is drained from the fracture. Fig. 3 shows one of the fracture surfaces and the water drain platen. Water outlet in the water drain

platen is divided into 10 ports and these ports are numbered by ① to ⑩. Thus, the heterogeneity of the water flow in the fracture can be evaluated.

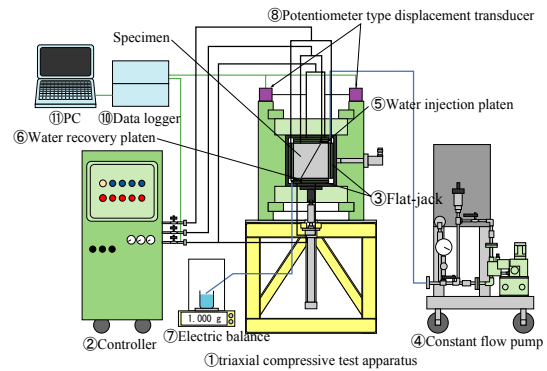


Fig. 1 Experimental system.

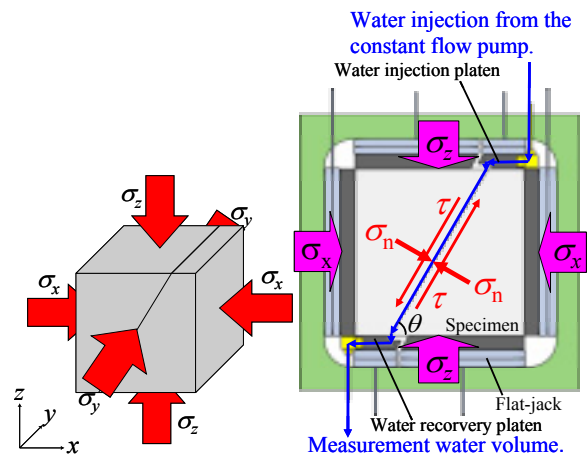


Fig. 2 Coordinate system and stress state in experiment.

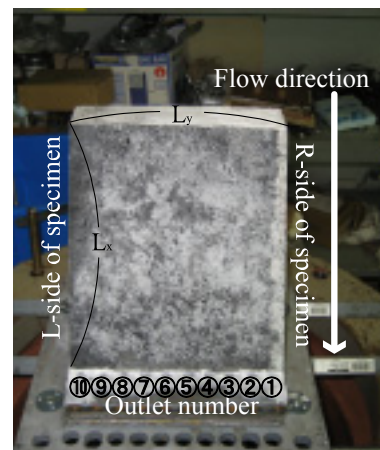


Fig. 3 Outlet of water.

## 2.2 Specimen

Fig. 4 shows schematic diagrams of the specimen. The specimen is cubic with one side of 250 mm long. The specimen has a fracture with an inclination angle  $\theta$  of  $60^\circ$  and is made of granite and mortar. The Surface heights and the aperture distribution of the fracture have been measured by Tomono (2001, Tomono) [2]. The length of the boundary perpendicular to the flow is denoted by  $L_y$  and parallel to the flow is denoted by  $L_x$ .

## 2.3 Procedure for estimating permeability

In this study, mass permeability  $M_p$  is defined by equation (1) to evaluate the heterogeneous water flow from measured water volume drained from each outlet port.

$$M_p = \frac{M_w}{\Delta p \cdot t} \quad (1),$$

where  $M_w$  is the water volume drained from each outlet port,  $\Delta p$  is pore pressure, and  $t$  is measurement time.

The hydraulic aperture  $e_h$  and the permeability  $k$  of the fracture are evaluated by equations (2) and (3) [3]:

$$e_h = \left\{ \frac{12\mu Q}{L_y \Delta p / L_x} \right\}^{\frac{1}{3}} \quad (2),$$

where  $\mu$  is the viscosity of water,  $Q$  is the volume flow rate, and

$$k = \frac{e_h^2}{12} \quad (3).$$

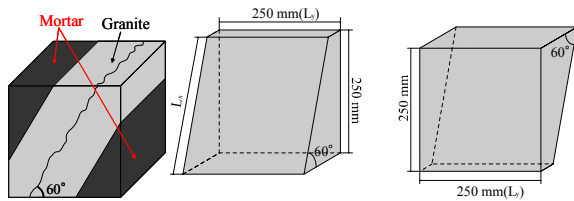


Fig. 4 Schematic diagrams of specimen.

## 3. IMPROVEMENT OF EXPERIMENTAL SYSTEM

Specimen must be sealed to prevent water from flowing out from the fracture except the outlet ports. One of the problems in the previous experimental system is weak seal for the specimen. Therefore, a new sealing method was developed as shown in Fig. 5. In this figure, RTV is the silicone which becomes like rubber at room temperature and KE-45 is paste-shaped silicone glue. The performance of the seal was improved by this method.

Another problem is that air is left in the fracture before experiments. The existence of air was confirmed by the observation of the fracture surfaces after the permeability test and thus, the remaining air interfered water flow in the fracture. Therefore, in this study, water was injected into the fracture from the bottom of the specimen to exhaust air out of the fracture before experiments.

The last problem is to control a decrease of the load. In this experimental system, the specimen is loaded by flat-jacks, and a relief valve is installed to decrease the inner pressure of the flat-jacks. However, it was difficult to precisely the control the inner pressure of the flat-jacks by the relief valve. Therefore, a metering valve was installed to control decreasing the inner pressure of the flat-jacks and it enabled to control decreasing loading stress precisely.

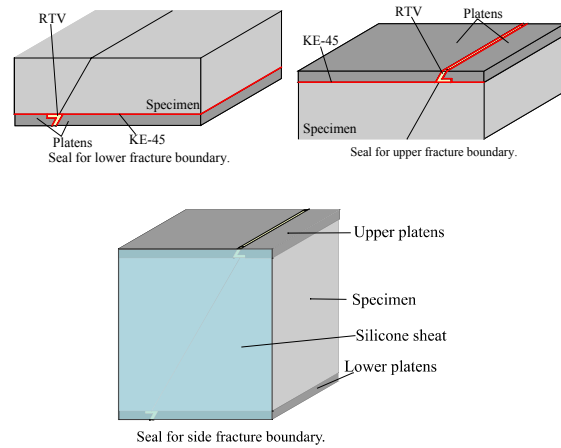


Fig. 5 Improved sealing method.

## 4. RESULTS AND DISCUSSIONS

Fig. 6 shows the changes in the stresses ( $\sigma_x$ ,  $\sigma_y$ ,  $\sigma_z$ , normal stress  $\sigma_n$  and shear stress  $\tau$ ), the pore pressure  $\Delta p$  and the shear displacement  $\delta$  with time in a permeability test. The permeability test started under the condition of a hydrostatic pressure of 5MPa. The initial pore pressure was 0.06 MPa. Shear stress  $\tau$  increases while normal stress  $\sigma_n$  is kept constant by controlling  $\sigma_z$  and  $\sigma_x$ . Shear displacement  $\delta$  increases with the shear stress  $\tau$ . Permeability tests were carried out 10 times including that in hydrostatic pressure, as indicated by red dotted lines in Fig. 6.

Fig. 7 shows the relation between the shear displacement and the mass permeability  $M_p$ . The numbers of from ① to ⑩ indicate the outlet

ports shown in Fig. 3. With no shear displacement, the values of  $M_p$  at the outlets varied in place by place, which showed that the water flow in the fracture is heterogeneous without shear. All values of  $M_p$  change little with the shear displacement for this fracture until the shear displacement is equal to 7.1 mm. This indicates that channeling flow developed little during the period. When the shear displacement exceeded 7.1 mm,  $M_p$  at some port increased and that at other ports decreased. This means that channels developed and this tendency became stronger with an increase in the shear displacement. The values of  $M_p$  at outlets ①, ②, ③ and ⑥ showed a tendency to increase, which indicated that the channels developed nearby these outlet ports. On the other hand, the values of  $M_p$  at outlets ⑦ and ⑧ showed a tendency to decrease, which indicates that channels disappeared nearby these outlet ports. Thus, water flow became more heterogeneous and also was localized as the shear displacement increased. All values of  $M_p$  decreased to nearly zero when the shear displacement exceeded 15 mm. This means that water flow parallel to the shear displacement was almost completely inhibited when the shear displacement exceeded 15 mm for this fracture.

Fig. 8 shows the contour map of the aperture distribution with the shear displacement when the fracture is closed to have a mean aperture of 3.0 mm. The area colored in black shows that the fracture surfaces are in contact each other, the area colored in white shows that the aperture is more than 4 mm, and the area colored between them shows that the aperture is greater as the color becomes warmer.

When the shear displacement reaches 6 mm, the areas where the aperture is greater than 4 mm spread widely. But the development of channels cannot be confirmed. This tendency is consistent with the result of the permeability test when the fracture was sheared by from 0 mm to 7.1 mm. Namely, distinct channels hardly developed with shear displacement that is equal to or smaller than 7.1 mm for this fracture. With an increase in the shear displacement, the areas where the aperture is more than 4 mm are connected to each other, and the areas with small apertures and with large apertures are more localized. Moreover, the areas where the surfaces are in contact each other form in the direction perpendicular to the shear displacement and these areas increases with the

shear displacement. Thus, this change in the aperture distribution made water flow more heterogeneous and localized as the shear displacement increases, which caused the change in the values of  $M_p$  at the outlets. When the shear displacement reaches 16 mm, the areas where the fracture surfaces are in contact each other are distributed widely around the center of the fracture surfaces and form a large ridge in the direction perpendicular to the shear displacement. It was considered that this ridge inhibited water flow in the direction parallel to the shear displacement and caused the decrease in all values of  $M_p$ .

Fig. 9 shows the relation between the shear displacement and the permeability  $k$ . The permeability  $k$  was almost constant until the shear displacement reached 13.4 mm and decreased when the shear displacement was more than 13.4 mm. Thus, the development of the channels and the heterogeneity in the water flow are not closely related to the change in the permeability  $k$  of the fracture until the shear displacement exceeded 13.4 mm. The formation of ridges perpendicular to the shear displacement caused the decrease in the permeability  $k$ .

Fig. 10 shows one of the fracture surfaces and the water drain platen after the test. Powder of the granite like clay minerals was distributed on both the fracture surfaces and the water drain platen. In particular, much powder existed around the areas where the fracture surfaces were in contact each other. Thus, an accumulation of debris produced by broken asperities in the fracture seriously contributes to the decrease in the permeability.

## 5. CONCLUSIONS

In this study, permeability tests with shear displacement were carried out using the triaxial compressive apparatus. Main results obtained in this study are summarized as follows:

- 1) The experimental system developed in the previous study was improved and the characteristics of the permeability of a tensile fracture with shear deformation were successfully evaluated by this improved experimental system.
- 2) Water flow becomes more heterogeneous as the shear displacement increases.
- 3) In this study, the permeability  $k$  was almost constant until the shear displacement exceeded 13.4 mm and decreased when the

shear displacement exceeded 13.4 mm. Formation of ridges perpendicular to the shear displacement with the shear displacement caused the dramatic decrease in the permeability  $k$ .

- 4) Accumulation of the debris in the fracture also causes a decrease in the permeability.

### REFERENCE

[1] Takanisi, 2005, Experimental study of the evaluation of permeability of a fracture with shear deformation under triaxial compressive stress, Tohoku Univ. Master Thesis.  
 [2] Tomono 2001, Shapes of fracture surface and size effects of aperture. Tohoku Univ. Master Thesis.  
 [3] Brown, S.R. : JGR, 92, 1337-1347, (1987)  
 Times New Roman 11 Point

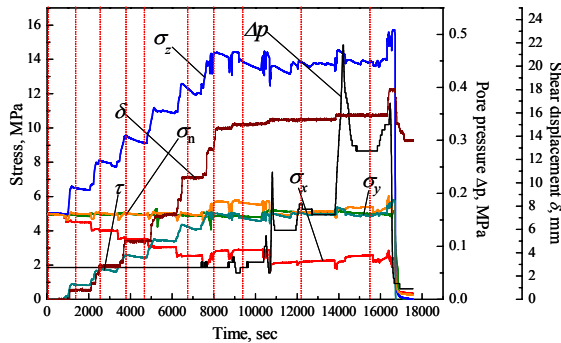


Fig. 6 Changes in stresses, pore pressure, and shear displacement with time.

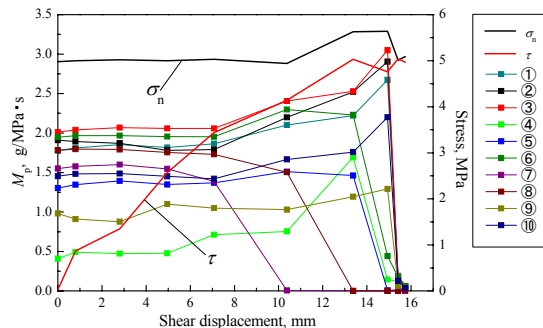


Fig. 7 Relation between shear displacement and mass permeability.

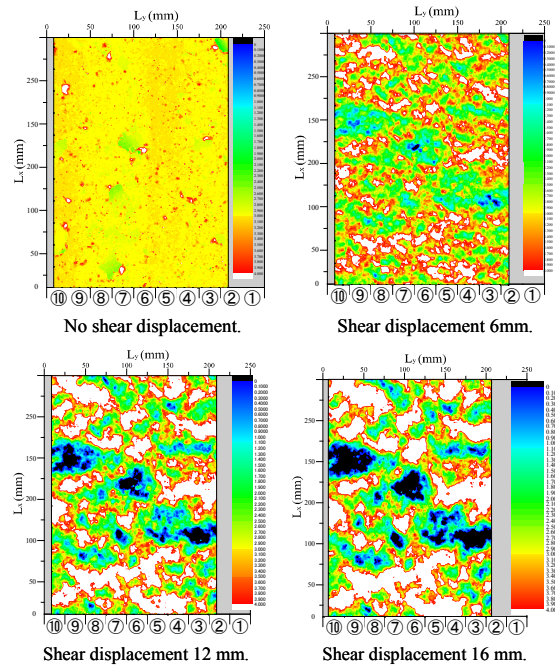


Fig. 8 The counter map of the aperture distribution with shear deformation when the fracture is closed to have a mean aperture of 3.0 mm.

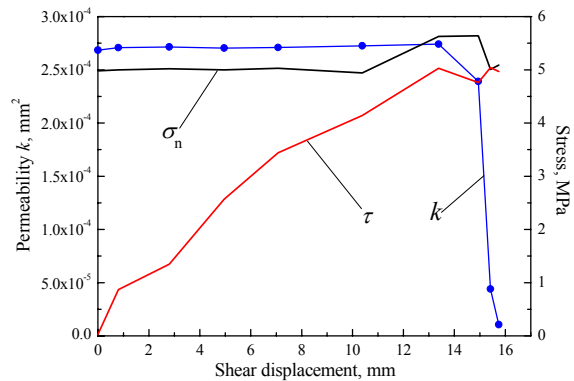
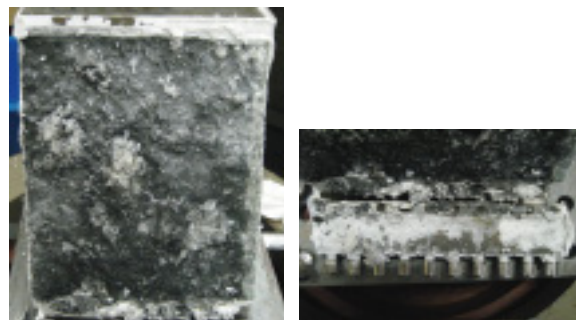


Fig. 9 Relation between shear displacement and permeability.



Fracture surface after experiment. Water recovery platen after experiment.  
 Fig. 10. Fracture surface after experiment and water recovery platen after experiment.